Laser Beam Cladding of Seating Surfaces on Exhaust Valves

Laser beam cladding significantly improves impact and wear resistance of valve seating surfaces compared to other surfacing methods

BY W. AIHUA, T. ZENGYI AND Z. BEIDI

ABSTRACT. The seating surfaces of internal exhaust valves were laser beam clad with Ni-Cr-B-Si and Co-Cr-W self-fluxing alloy powders using a 2 kW, CW CO_2 laser. Compared to traditional techniques, such as plasma spray and vacuum induction fusing methods, laser beam cladding is free from porosity and cracks, has a finer dendrite microstructure, a more narrow heat-affected zone, and a higher microhardness value. A thermal impact wear test simulating the forced condition of exhaust valves on the seating surfaces shows that laser-clad (LC) Ni-Cr-B-Si alloy at a high laser beam transverse speed produces better thermal impact wear resistance than LC surfacing at low laser beam transverse speed or plasma sprayed (PS) and vacuum induction fused (VIF) surfacing. The reason for this is the laser cladding's higher microhardness value, finer microstructure and the precipitation of hard phase particles (Ni_3B and $Cr_{23}C_6$) at the tested temperature of about 780°C (1436°F). Laser beam clad valves with Ni-Cr-B-Si alloy powder have been tested in an internal combustion engine.

KEY WORDS

Sealing Surfaces
Exhaust Valves
Laser Beam Cladding
Microstructure
Thermal Impact
Wear Resistance
Microhardness
Clad Coatings
Alloy Powders
Porosity

W. AIHUA, T. ZENGYI and Z. BEIDI are with the Mechanical Engineering Department, Huazhong University of Science and Technology, Wuhan, China.

Introduction

Exhaust valves used for internal combustion engines are subjected to wear and corrosion at high temperatures of 600° to 800°C. Pitting and spalling occur on the seating surfaces after valves have been in service under the above conditions for a short time, affecting the efficiency of engines. Various processes such as plasma spraying of alloy powder and vacuum induction fusing of preplaced alloy powder have been used to apply surfacing materials onto the seating surface of exhaust valves to improve seating properties. But the service life of valves is still not long enough, for these claddings have poor wear and corrosion resistance and the rate of finished products is low due to porosity and cracks existing in the claddings.

Since 1974, laser beam cladding has been used to improve the wear and corrosion resistance of materials. The first industrial use of lasers in cladding was done by Rolls Royce in 1981, when it clad turbine blade shroud interlocks on the RG 211 engine (Ref. 1). One reason for the great industrial interest in this process is because it is one of the very few surfacing processes that causes little thermal damage to the substrate and relatively slight distortion. Laser beam cladding techniques were used to improve the properties of the coating and the service life of internal exhaust valves.

Experimental Procedure

Laser beam cladding experiments were performed with Ni-Cr-B-Si and Co-Cr-W self-fluxing alloy powders, which are commonly used in the plasma spraying process and the vacuum induction fusing process. The composition of the powders is shown in Table 1. Powders were applied to the seating surface of the valve with an or-

Table 1—Composition of Powders Used in the Experiment (wt-%)

Powder	C	Si	B	Cr	Fe	Ni	W	Co	Powder Size (mesh)
Ni-Cr-B-Si	0.65–0.75	3.0–4.0	2.0–3.0	25–26.5	≤5	bal	–	–	−60 to +200
Co-Cr-W	0.7–1.4	0.7–2.0	0.5–1.2	26–32	≤5	–	1.0–6.0	bal	−60 to +200

Table 2—Parameters of LC, PS and VIF Claddings

Sample Number	Alloy Powder	Cladding Method	Transverse Speed for Laser Cladding (mm/s)	Thickness of Preplaced Powder (mm)
1	Ni-Cr-B-Si	LC	2.8	2.2
2	Ni-Cr-B-Si	LC	4.7	2.2
3	Ni-Cr-B-5i	LC	7.2	2.2
4[a]	Ni-Cr-B-Si	PS	–	2.2
5	Co-Cr-W	LC	2.8	2.2
6	Co-Cr-W	LC	4.7	2.2
7	Co-Cr-W	LC	7.2	2.2
8[a]	Co-Cr-W	VIF	–	2.2

(a) The samples selected for experiments were clad with the optimum PS or VIF parameters used for production in many factories in China.

Fig. 1 — Cross-section of LC cladding with Ni-Cr-B-Si alloy. A — Heat-affected zone-cladding interface region, transverse speed of 2.8mm/s; B — surface cladding, transverse speed of 2.8 mm/s; C — surface cladding, transverse speed of 7.2 mm/s (300X).

ganic binder (the composition of the valve steel used as substrate is Fe-0.5C-21Cr-9Mn-4Ni-N) prior to laser processing. For this investigation, the laser was operated at the power of 2 kW, the laser beam was defocused to 5 mm (0.2 in.) in diameter, and valves were spun at a linear speed of 2.8 to 7.2 mm/s (0.11 to 0.28 in./s), using a rotating device. The designation of samples is shown in Table 2. A coaxial N_2 gas was used to shield the pool from oxidation and to prevent the focusing lens from being fogged by fumes.

Microstructural investigations of clad surfacings were carried out by means of an optical microscope, scanning electron microscope, x-ray structure analyzer and transmission electron microscope. A thermal impact wear test was also carried out according to the forced condition of the seating surface to compare the resistance of three kinds of cladding: LC, PS and VIF.

Results and Discussion

Micro Check of Cladding

Clad seating surfaces and cross-sections of claddings were visually inspected and examined with a low-power light microscope. Results show that LC Ni-Cr-B-Si claddings are free from porosity and cracks, and LC Co-Cr-W claddings are free from porosity, but cracks exist when the transverse speed exceeds 4.7 mm/s (0.18 in./s). The direction of cracks is perpendicular to the direction of transverse speed. Plasma spray surfacing shows apparent porosity and cracks, while VIF surfacing shows porosity. Furthermore, the investigation showed that the porosity in PS surfacing mainly exists in the closed area due to the changeable intensity of plasma at its beginning and end. The porosity in the VIF surfacing resulted from the poor fluidity of melted powder. Since the laser beam heats the preplaced powder more efficiently and causes fluid flow in the weld pool (Ref. 2), it may eliminate porosity. Also, there is no porosity in the closed area with the laser because the powder remained unchanged during the whole process. The cracks in the LC surfacing produced at higher transverse speeds are induced by the brittleness of Co-Cr-W alloy, and greater thermal stress remained in these claddings.

Microstructure

Laser cladding can be divided into three morphologies: dendrite in the clad region, equiaxial grain in the interfacial region and coarse austenite in the heat-affected region, as shown in Fig. 1. Solidifying morphology is determined by temperature gradient G and solidifying rate R, as shown in Fig. 2.

Using the theory that equiaxial grains in the interfacial region form due to a very large temperature gradient G and a very low solidifying rate R, then the solid/liquid interface moves away from the interfacial region in conjunction with reduced G and increased R. The solidification morphology changes into dendrite in the postsolidifying cladding.

Another important phenomenon can be found in Figs. 1A, 1B and 3. The dendrite gets finer from interface to surface and the dendrite of the cladding becomes finer with the increase in transverse speed. It can be explained by the following formula:

$$d = \beta\,(GR)^{-1/3} = \beta\,(\dot{T})^{-1/3} \quad (4)$$

Where β is a coefficient, $\dot{T}$ is the cooling rate of fluid, and d is the arm of dendrite. Being adjacent to the surface of the coating and increasing the transverse speed both enlarges the cooling $\dot{T}$ and produces a finer dendrite structure.

X-ray diffraction analyses show the main phases of cladding: FCC Ni-Cr-based solid solution and Cr_7C_3 in the LC Ni-Cr-B-Si surfacing, and FCC Co-Cr-based solid solution, Cr_7C_3 and Cr_2B in the LC Co-Cr-W surfacing.

Compared with PS and VIF surfacing, LC surfacing has a finer dendrite structure (Figs. 1B, 1C, 3 and 4), a more narrow heat-affected zone and less dilution of the base metal (Table 3) because the laser beam has high density power and it heats the preplaced powder directly.

Microhardness and Thermal Impact Test

The variations in hardness of LC, PS and VIF surfacing are shown in Fig. 5 as a function of distance from the surface. The mi-

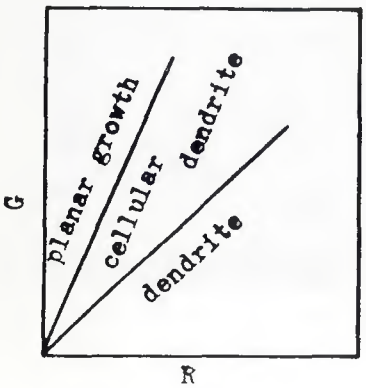

Fig. 2 — Diagram of solidifying morphology affected by G and R.

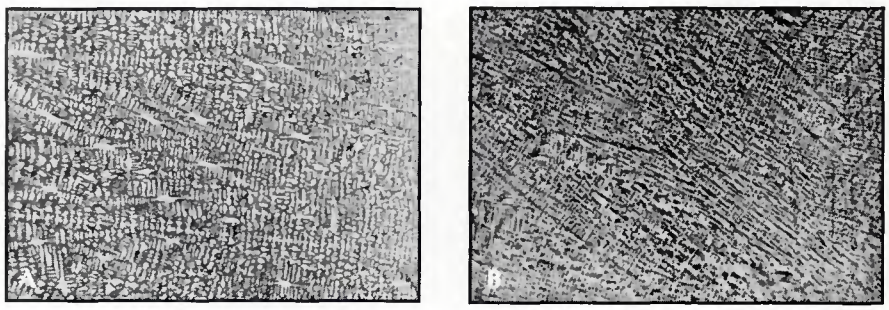

Fig. 3 — Surface microstructure of LC cladding with Co-Cr-W alloy. A — Transverse speed of 2.8 mm/s; B — transverse speed of 7.2 mm/s (300X).

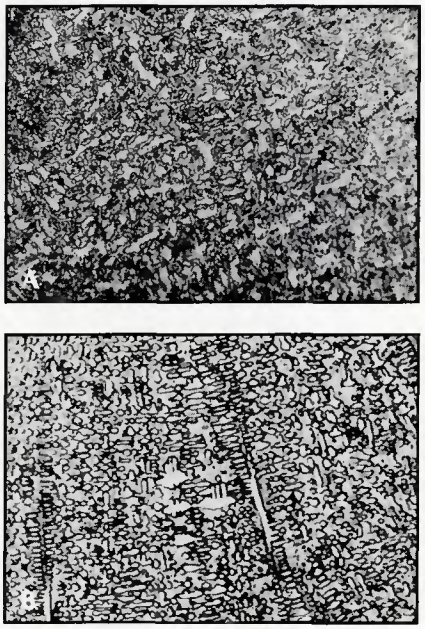

Fig. 4 — Optical micrographs of surface cladding. A — Ni-Cr-Si cladding applied by PS; B — Co-Cr-W cladding applied by VIF (300X).

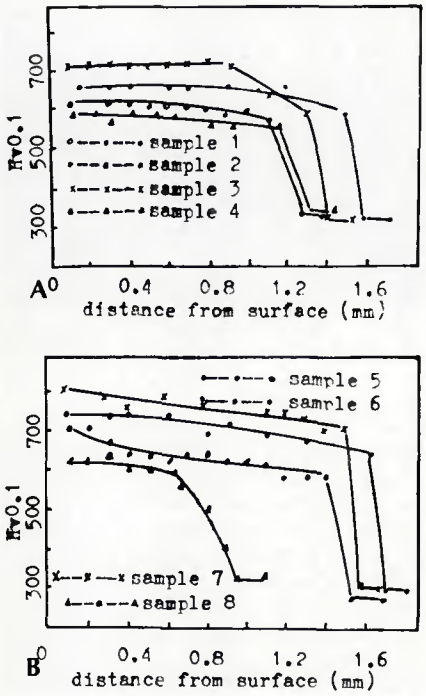

Fig. 5 — Variations in microhardness below the surface. A — Ni-Cr-B-Si cladding; B — Co-Cr-W cladding.

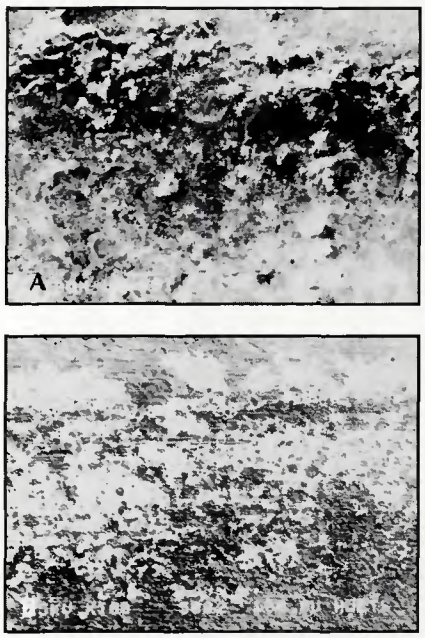

Fig. 6 — A — Surface morphology of tested samples; B — seating surface of valves damaged in engines.

crohardness of LC coatings is enhanced with the increase in transverse speed. The microhardness of LC Ni-Cr-B-Si coatings and LC Co-Cr-W coatings is higher than that of PS Ni-Cr-B-Si coating and VIF Co-Cr-W coating, respectively, because the finer dendrite microstructure increases microhardness value. The LC Co-Cr-W coatings show a higher microhardness than LC Ni-Cr-B-Si coatings at the same transverse speed due to the difference in composition, but the LC Ni-Cr-B-Si coatings can get higher microhardness values over VIF Co-Cr-W coatings.

A thermal impact wear test was carried out on a thermal impact wear tester we made. The head of the valve is heated to 780°C (the approximate maximum service temperature of an exhaust valve) using the induction heating method. The valve seat was then driven by the cylinder, and impact occurred between the seating surface of the valve and the valve seat in air. The impact force was 841 N (189 lbf) and the impact frequency was 18 cycles per minute in this experiment. After the head of the valve had impacted the valve seat for 2000 cycles, pitting and spalling on the seating surface occurred, which closely compares to seating surface damage in engines — Fig. 6. This result proved that the simulation test was successful (Ref. 5).

The surface profiles of tested samples were analyzed using an electron microscope. The main mechanisms of thermal impact wear are fatigue, friction and abrasion.

Furthering the investigation, the thermal impact wear resistance was evaluated by measuring the impact wear width on the

Table 3—The Comparison of Heat-Affected Zone and Dilution Width

Sample number	1	2	3	4	5	6	7	8
Heat-affected zone (μm)	210	58	36	235	118	48	36	360
Dilution width (μm)	192	100	57	239	132	75	70	125

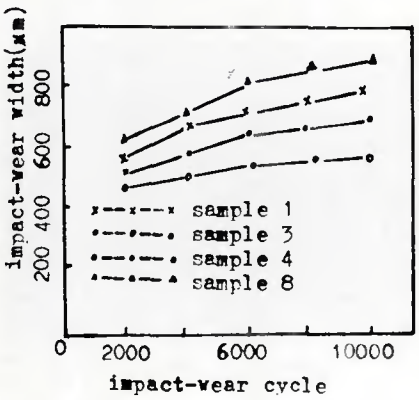

Fig. 7 — Impact wear width vs. impact wear cycle.

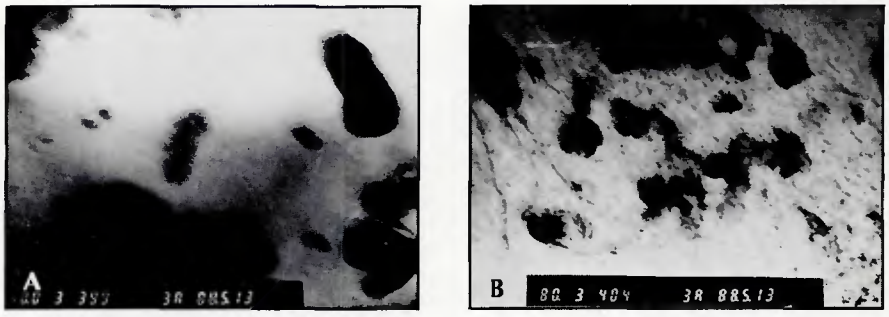

Fig. B — TEM micrographs showing the precipitated phases for LC cladding with Ni-Cr-B-Si alloy at the transverse speed of 7.2 mm/s. The sample was tested for 10,000 cycles. A — $Cr_{23}C_6$ (60,000X); B—Ni_3B (80,000X).

Table 4—Increase in Microhardness after Samples Were Tested for 10,000 Cycles

Sample number	1	3	4	8
Increase in microhardness (HV)	30	150	90	0

seating surface of tested samples—Fig. 7. Impact wear width was affected by microhardness, microstructure and phase structure in the surfacing. Results show that LC Ni-Cr-B-Si surfacing at a transverse speed of 7.2 mm/s (0.28 in./s) possess the minimum impact-wear width or the best thermal impact wear resistance among all surfacing. The variation of microhardness for several samples is shown in Table 4 after samples were tested for 10,000 cycles. The increase in microhardness in these surfaces resulted from the precipitation of Ni_3B and $Cr_{23}C_6$ in the coatings with a supersaturated solid solution. The distribution of Ni_3B and $Cr_{23}C_6$ is illustrated in Fig. 8.

The supersaturated solid solution results from the fast cooling rate of fluid in the processing. Sample 3 is characterized by the highest increase in microhardness among tested samples because of its response to the greatest cooling rate, which causes the highest supersaturated solid solubility. It is clear that the fine microstructure and the precipitation of Ni_3B and $Cr_{23}C_6$ are the main reasons for improving the impact wear resistance.

The exhaust valves clad by laser beam using the parameters of Number 3 (Table 2) were tested in an internal combustion engine under the condition of full speed and full load for 300 h. Results show that wear and corrosion resistance of the valve seating surface improved by three to four times in comparison with other processes. Laser cladding on the seating surface of the valve can be used successfully in practice.

Conclusions

1) Laser cladding (LC) on the seating surface of exhaust valves was developed to avoid discontinuities such as porosity and cracks found in plasma spray (PS) or vacuum induction fused (VIF) surfacing.

2) A coating with finer microstructure, more narrow heat-affected zone and higher microhardness value can be obtained with the laser cladding technique when compared to PS or VIF surfacing.

3) Impact wear test and engine test both show that laser-beam-clad Ni-Cr-B-Si alloy on the seating surface of exhaust valves can improve the properties of valves compared to PS and VIF methods. It is a valid process to increase the service life of internal combustion engine exhaust valves.

Acknowledgments

The authors are grateful for the financial support of the State Education Commission of China under Contract No. 75-72-05-01-18. We also appreciate the assistance of Zeng Xiaoyian with the laser processing experiment and Associate Prof. Shao Zhongyi with the thermal impact wear test.

References

1. Metzbower, E. A. 1983. *Laser in Materials Processing*: Published by ASM International, Materials Park, Ohio. pp. 230–240.

2. Anthoney, T. R., and Cline, H. E. 1977. Surface rippling induced by surface-tension gradients during laser surface melting and alloying. *Journal of Applied Physics* 48(9): 3888–3894.

3. Ashbrook, R. L. 1983. *Rapid Solidification Technology*. ASM International, Materials Park, Ohio.

4. Hanqi Hu. 1983. *Solidification of Metals*, pp. 180–214. Metallurgical Industry Press. (in Chinese).

5. Ha Bixi, K-H. 1987, *Wear and Hardness of Materials* 45, 88. Mechanical Industry Press, pp. 45, 88 (in Chinese).

WRC Bulletin 343
May 1989

Destructive Examination of PVRC Weld Specimens 202, 203 and 251J

This Bulletin contains three reports:

(1) Destructive Examination of PVRC Specimen 202 Weld Flaws by JPVRC
By Y. Saiga

(2) Destructive Examination of PVRC Nozzle Weld Specimen 203 Weld Flaws by JPVRC
By Y. Saiga

(3) Destructive Examination of PVRC Specimen 251J Weld Flaws
By S. Yukawa

The sectioning and examination of Specimens 202 and 203 were sponsored by the Nondestructive Examination Committee of the Japan Pressure Vessel Research Council. The destructive examination of Specimen 251J was performed at the General Electric Company in Schenectady, N.Y., under the sponsorship of the Subcommittee on Nondestructive Examination of Pressure Components of the Pressure Vessel Research Committee of the Welding Research Council. The price of WRC Bulletin 343 is $24.00 per copy, plus $5.00 for U.S., or $8.00 for overseas, postage and handling. Orders should be sent with payment to the Welding Research Council, Room 1301, 345 E. 47th St., New York, NY 10017.

WRC Bulletin 355
July 1990

Programming and Control of Welding Processes—Experience of the USSR

By V. Malin

This report is an in-depth look at technical welding studies and their implementation in the USSR, a country that has a long history of welding automation development. More than 300 articles published in the USSR over the last three decades were examined, and 177 are referenced in this report.

Publication of this report was sponsored by the Interpretive Reports Committee of the Welding Research Council. The price of WRC Bulletin 355 is $35.00 per copy, plus $5.00 for U.S. and $10.00 for overseas postage and handling. Orders should be sent with payment to the Welding Research Council, 345 E. 47th St., Room 1301, New York, NY 10017.

WRC Bulletin 358
November 1990

The Effect of Crack Depth to Specimen Width Ratio on the Elastic-Plastic Fracture Toughness of a High-Strength Low-Strain Hardening Steel

By J. A. Smith and S. T. Rolfe

An experimental and analytical study of square three-point bend specimens was conducted to investigate the elastic-plastic fracture toughness of a high-strength low-strain hardening steel using shallow and deep crack test specimens. Changes in CTOD level with varying crack depth-to-width ratios of CTOD specimens were investigated for this material and compared to other results to determine how material properties, such as the strength level and strain hardening, affect the CTOD level for varying a/W ratios.

Publication of this report was sponsored by the Pressure Vessel Research Council of the Welding Research Council and the American Iron and Steel Institute. The price of WRC Bulletin 358 is $25.00 per copy, plus $5.00 for U.S. or $10.00 for overseas postage and handling. Orders should be sent with payment to the Welding Research Council, 345 E. 47th St., Room 1301, New York, NY 10017.

WRC Bulletin 359
December 1990

Weldability of Low-Carbon Micro-Alloyed Steels for Marine Structures

By C. D. Lundin, T. P. S. Gill, C. Y. P. Qiao, Y. Wang and K. K. Khan

This report covers the "Validity of Carbon Equivalent Formulae," a "Prediction of HAZ Hardness," a "Calculation of Cooling Rate/Cooling Time," "Hydrogen Sensitivity and Cracking Morphology," "HAZ Softening," and presents a large number of "HAZ Microstructures."

Publication of this document was sponsored by the U.S. Interagency Ship Structure Committee and the Welding Research Council. The price of WRC Bulletin 359 is $45.00 per copy, plus $5.00 for U.S. or $10.00 for overseas shipping and handling. Orders should be sent with payment to the Welding Research Council, 345 E. 47th St., Room 1301, New York, NY 10017.